# Relating the Drag Coefficient and the Roughness Length over the Sea to the Wavelength of the Peak Waves

EDGAR L ANDREAS

*NorthWest Research Associates, Inc., Lebanon, New Hampshire*

(Manuscript received 25 November 2008, in final form 26 May 2009)

ABSTRACT

The standard 10-m reference height for computing the drag coefficient over the sea is admittedly arbitrary. The literature contains occasional suggestions that a scaling length based on the wavelength of the peak waves $\lambda_p$ is a more natural reference height. Attempts to confirm this hypothesis must be done carefully, however, because of the potential for fictitious correlation between nondimensional dependent and independent variables. With the DMAJ dataset as an example, this study reviews the issue of fictitious correlation in analyses that use $\lambda_p/2$ as the reference height for evaluating the drag coefficient and that use $k_p$ $(=2\pi/\lambda_p)$ as a scale for the roughness length $z_0$. (The DMAJ dataset is a compilation of four individual datasets; D, M, A, and J, respectively, identify the lead authors of the four studies: Donelan, Merzi, Anctil, and Janssen.) This dataset has been used in several previous studies to evaluate the dependence of $k_p z_0$ and the drag coefficient evaluated at $\lambda_p/2$ on the nondimensional wave parameter $\omega_* = \omega_p u_*/g$. Here $\omega_p$ is the radian frequency of the peak in the wind–wave spectrum, $u_*$ is the friction velocity, and $g$ is the acceleration of gravity. Because the DMAJ dataset does not, however, include independent measurements of $\lambda_p$ and $\omega_p$, $\lambda_p$ had to be inferred from measurements of $\omega_p$ through the wave dispersion relation. The presence of $\omega_p$ in both the dependent and independent variables, therefore, exacerbates the fictitious correlation. One conclusion, thus, is that using $\lambda_p$ to formulate the drag coefficient and the nondimensional roughness length as functions of a nondimensional variable that includes $\omega_p$ requires a dataset with independent measurements of $\lambda_p$ and $\omega_p$.

## 1. Introduction

"The study of error is not only in the highest degree prophylactic, but it serves as a stimulating introduction to the study of truth." —Walter Lippmann

The idea of basing the drag coefficient over the ocean on a reference wind speed evaluated at a height determined by the properties of the wind waves has merit. After all, the standard 10-m reference height is occasionally under water in high winds.

The literature contains periodic discussions of using the wind speed evaluated at a reference height based on the wavelength of the peak of the wavenumber spectrum of the wind waves $\lambda_p$ for parameterizing wave growth and drag over the ocean (Al-Zanaidi and Hui 1984; Donelan and Pierson 1987; Pierson 1990; Resio et al. 1999; Oost et al. 2002; Hwang 2004, 2005a,b,c, 2006). Most of these studies also use another wave parameter, such as $\omega_p$, the radian frequency of the peak in the wave frequency spectrum, to create nondimensional variables. If $\lambda_p$ and $\omega_p$ are not measured independently, however, such analyses can suffer from fictitious correlation.

As an example of such hazards, I reanalyze the DMAJ dataset, which is a compilation from data tables included in the papers by Donelan (1979), Merzi and Graf (1985), Anctil and Donelan (1996), and Janssen (1997). The DMAJ dataset has been used previously to investigate the behavior of an air–sea drag coefficient evaluated at $\lambda_p/2$ and the benefits of scaling the roughness length $z_0$ with $k_p$ $(=2\pi/\lambda_p)$ (Hwang 2004, 2005a,b,c). In these studies, both $k_p z_0$ and the drag coefficient evaluated at $\lambda_p/2$ were plotted against the nondimensional wave parameter $\omega_* = \omega_p u_*/g$, where $u_*$ is the friction velocity and $g$ $(=9.81\ \mathrm{m\ s^{-1}})$ is the acceleration of gravity. In both plots, the correlation was remarkably tight; the analyses therefore seemed to prove the value of $\lambda_p$ scaling.

Unfortunately, the DMAJ dataset was not adequate for these analyses. It contains no direct measurements

*Corresponding author address:* Dr. Edgar L Andreas, NorthWest Research Associates, Inc. (Seattle Division), 25 Eagle Ridge, Lebanon, NH 03766-1900.
E-mail: eandreas@nwra.com

DOI: 10.1175/2009JPO4189.1

of $\lambda_p$; hence, $\lambda_p$ values in the dataset came from measurements of $\omega_p$ through the dispersion relation for wind waves,

$$\omega^2 = gk \tanh(kD), \tag{1.1}$$

where $\omega$ is the wave frequency, $k$ is the wavenumber, and $D$ is the water depth. As a result, the dependent variables—$k_p z_0$ and the neutral-stability drag coefficient evaluated at $\lambda_p/2$, $C_{\mathrm{DN},\lambda_p/2}$—are based on some of the same values as the independent variable, $\omega_* = \omega_p u_*/g$. The correlations in scatterplots of these nondimensional variables are therefore largely fictitious and, thus, no proof for the validity of wavelength scaling.

Hicks (1978a, 1978b, 1981) and Kenney (1982) first alerted the oceans and atmospheres community to the hazards of fictitious correlation 30 years ago, but the medical community has known about the problems created by using the same variable for scaling both dependent and independent variables for a hundred years (Pearson 1897; Pearson et al. 1910). With the DMAJ dataset as an example, I review the general problem of fictitious correlation and how to mathematically evaluate its potential effect. I do this by developing equations that predict the best fits for $C_{\mathrm{DN},\lambda_p/2}$ and $k_p z_0$ as functions of $\omega_*$ under the assumption that none of the measured variables are correlated. Lines fitted to scatterplots that are based on this analysis are little different from lines based on the actual data.

Randomly scrambling the $k_p$ values in the DMAJ dataset reiterates the effects of the fictitious correlation: plots of both $C_{\mathrm{DN},\lambda_p/2}$ and $k_p z_0$ versus $\omega_*$ still have good correlation because of the shared variables.

These analyses also imply requirements for the specific problem of testing the validity of wavelength scaling for parameterizing air–sea drag or wind–wave growth. Because the wavelength at the peak of the wavenumber spectrum is the key variable in such studies, it should be directly measured.

## 2. The DMAJ dataset

The sources in the DMAJ dataset include Donelan (1979) and Anctil and Donelan (1996), who collected their data in the west end of Lake Ontario; the water depth was 12 m in the former set and ranged from 2 to 12 m in the latter set. Merzi and Graf (1985) made their measurements in Lake Geneva (Switzerland) in water that was 3 m deep. Janssen (1997) obtained his data in the North Sea in water 18 m deep.

All four sources tabulate eddy-covariance or profile measurements of the friction velocity. All four sources also include $U_{N10}$, the wind speed at a reference height of 10 m with stratification effects removed. I refer to this variable as the neutral-stability, 10-m wind speed. From these data, the neutral-stability, 10-m drag coefficient is simply

$$C_{\mathrm{DN10}} = \left(\frac{u_*}{U_{N10}}\right)^2. \tag{2.1}$$

Furthermore, because in neutral stratification the wind speed profile obeys

$$U_N(z) = \frac{u_*}{\kappa} \ln\left(\frac{z}{z_0}\right), \tag{2.2}$$

where $z$ is the height and $\kappa$ (=0.40) is the von Kármán constant, the roughness length derives from

$$z_0 = 10 \exp\left(\frac{-\kappa U_{N10}}{u_*}\right). \tag{2.3}$$

Here, $z_0$ is in meters. Not all four of the sources tabulate $z_0$, but it can be calculated from (2.3) using the reported values of $u_*$ and $U_{N10}$.

Finally, on combining (2.1) and (2.2), we obtain the standard relationship between the drag coefficient and the roughness length:

$$C_{\mathrm{DN10}} = \left[\frac{\kappa}{\ln(10/z_0)}\right]^2. \tag{2.4}$$

Here, $z_0$ must be expressed in meters.

The DMAJ dataset is potentially useful for parameterizing air–sea momentum exchange because the individual sources also tabulate wave variables. In particular, they all report $\omega_p$; $f_p$ (=$\omega_p/2\pi$), the cyclic peak wave frequency; or $c_p$, the phase speed of the peak waves. From this latter value, $\omega_p$ was derived from the definition

$$\omega_p = k_p c_p \tag{2.5}$$

and the dispersion relation in (1.1).

None of the four sources, however, report the key variable for studying wavelength scaling, the wavelength of the peak waves. The values for $\lambda_p$ in the dataset therefore came from $\omega_p$ and the dispersion relation in (1.1). Once we have this quantity, however, we can use it in (2.1) and (2.2) to estimate the drag coefficient derived from the neutral-stability wind speed at a reference height of $\lambda_p/2$:

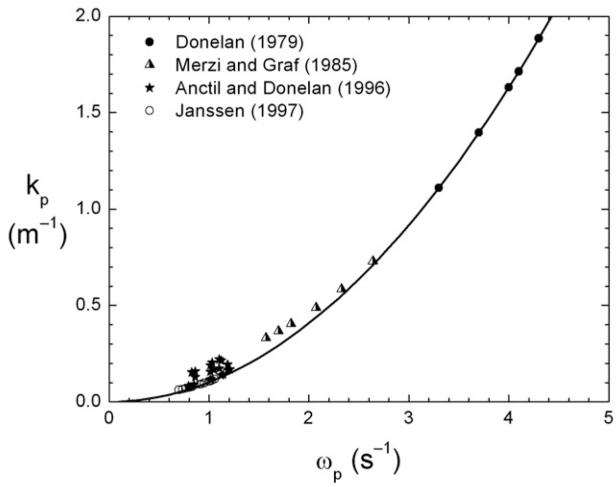


FIG. 1. Scatterplot of the peak wavenumber and the peak frequency from the DMAJ dataset. The curve is the deep-water dispersion relation in (2.7). The DMAJ dataset has 142 lines of data; many of these points do not show up as distinct markers here, though, because they have the same $\omega_p$ values and, thus, the same $k_p$ values. For example, the Merzi and Graf (1985) set contains 60 observations but only 6 appear in this plot because of duplications in $\omega_p$ (and therefore in $k_p$).

$$C_{\mathrm{DN},\lambda_p/2} = \left\{\frac{\kappa}{\ln[\pi/(k_p z_0)]}\right\}^2, \qquad (2.6)$$

where, remember, $k_p = 2\pi/\lambda_p$. In effect, these manipulations introduce one of the main independent variables, $\omega_p$, into the dependent variable.

The DMAJ dataset has also been used to explore scaling $z_0$ with $k_p$; plots of the nondimensional variable $k_p z_0$ versus $\omega_p u_*/g$ result. Again, $\omega_p$ occurs prominently in both dependent and independent variables.

Figure 1 compares the $\omega_p$ and $k_p$ values in the DMAJ dataset. The line in the figure is the deep-water dispersion relation:

$$\omega_p^2 = g k_p. \qquad (2.7)$$

Donelan's (1979) and Janssen's (1997) data follow this relation almost perfectly; both thus observed deep-water waves. Merzi and Graf's (1985) data deviate slightly from (2.7); their data reflect waves in transition between deep and shallow water. Most of Anctil and Donelan's (1996) observations were in shallow water, where depth effects cause their data to deviate most from (2.7).

The correlation in Fig. 1, however, is much too good for $\omega_p$ and $k_p$ to be independently measured geophysical quantities (cf. Donelan 1979). In fact, a plot (not shown) of the $\omega_p$ values in the DMAJ dataset against $\omega_p$ values computed from the dispersion relation (1.1) using the reported $k_p$ values is perfectly correlated. In other words, in the DMAJ dataset, $k_p$ comes from $\omega_p$ through the dispersion relation: they were not measured independently.

Several reasons exist for doubting that, in a natural environment, independently measured $\omega_p$ and $k_p$ values will follow (1.1) perfectly. Equation (1.1) is the linearized dispersion relation; its derivation presumes waves of small amplitude (e.g., Tucker and Pitt 2001, p. 25). Nonlinear (high amplitude or breaking) waves will cause discrepancies in (1.1). Second, currents cause Doppler shifts in $\omega$ such that it is no longer related to $k$ precisely as in (1.1) (Massel 2007, p. 41f; Pierson 1990). Third, because the wave field is an ensemble of many wave groups and amplitudes, identifying the peak in the frequency spectrum and the peak in the wavenumber spectrum is not without ambiguity.

Finally, Plant et al. (2005) state that the true peak wavenumber will always be smaller than the wavenumber related to the true peak frequency through (1.1). Plant (2009) proves this result. Briefly, because frequency $[F(\omega)]$ and wavenumber $[F(k)]$ spectra are related by (Tucker and Pitt 2001, p. 33f)

$$F(k) = \left(\frac{c_g}{k}\right) F(\omega), \qquad (2.8)$$

where $c_g$ is the group velocity, the actual relationship between $k_p$ and $\omega_p$ depends on the shape of the wave spectrum. As a result, any empirical $k_p$–$\omega_p$ relationship should demonstrate some randomness.

In light of these several complications, independently measured $\omega_p$ and $k_p$ values would not follow (1.1) or even the deep-water relation (2.7) exactly and would be more scattered than the values in Fig. 1.

## 3. Quantifying the fictitious correlation

Figure 1 hints at the shortcomings in the DMAJ dataset. Now I mathematically quantify the potential for fictitious correlation in plots of $C_{\mathrm{DN},\lambda_p/2}$ and $k_p z_0$ versus $\omega_p u_*/g$ when $\omega_p$ and $\lambda_p$ are not independent. Some of these mathematical techniques follow Hicks's (1978a) suggestions, though the methods in Andreas (2002) and Andreas et al. (2006) are closer to what I use here. In essence, the following analysis uses differentials or, in Margenau and Murphy's (1956, p. 504ff) terminology, "residuals."

Because of the range of values and the likelihood of a power-law relation between them, it is common to plot $\ln C_{\mathrm{DN},\lambda_p/2}$ versus $\ln\omega_*$ (e.g., Hwang 2004, 2005a,b,c). Likewise, I consider a plot of $\ln k_p z_0$ versus $\ln\omega_*$. For each plot, we look for a least squares fit to the scatterplot such that

$$y = ax + b, \tag{3.1}$$

where $y$ is the dependent variable—either $\ln C_{\mathrm{DN},\lambda_p/2}$ or $\ln k_p z_0$—and $x$ is the independent variable, $\ln\omega_*$. The fitting gives the best slope $a$ and intercept $b$.

In least squares linear regression, the slope comes from

$$a = \frac{\mathrm{cov}[x, y]}{\sigma_x^2}, \tag{3.2}$$

where $\sigma_x^2$ denotes the variance in $x$ and $\mathrm{cov}[x, y]$ indicates the covariance between $x$ and $y$. The intercept then derives from

$$b = \overline{y} - a\overline{x}, \tag{3.3}$$

where the overbars denote the averages of $x$ and $y$.

From pure mathematics, I can compute $a$ and $b$ from the DMAJ dataset under the assumption that none of the fundamental variables—$k_p$, $u_*$, $U_{N10}$, or $D$—are correlated. That is, the covariance between any two of these is assumed to be zero. In effect, this approach explores the mathematics of the analysis rather than the physics of the hypothesis that $k_p$ is a useful length scale.

### a. Plots of $C_{\mathrm{DN},\lambda_p/2}$ versus $\omega_p u_*/g$

To begin, I evaluate the relevant differentials. For $\ln\omega_*$, where

$$\omega_* = \frac{\omega_p u_*}{g}, \tag{3.4}$$

$$d(\ln\omega_*) = \frac{1}{\omega_*}\left(\frac{\partial\omega_*}{\partial\omega_p}\, d\omega_p + \frac{\partial\omega_*}{\partial u_*}\, du_*\right). \tag{3.5}$$

Here I have ignored any variation in $g$. Equation (3.4) yields the partial derivatives:

$$\frac{\partial\omega_*}{\partial\omega_p} = \frac{\omega_*}{\omega_p} \quad \text{and} \tag{3.6}$$

$$\frac{\partial\omega_*}{\partial u_*} = \frac{\omega_*}{u_*}. \tag{3.7}$$

Hence, (3.5) becomes

$$d(\ln\omega_*) = \frac{d\omega_p}{\omega_p} + \frac{du_*}{u_*}. \tag{3.8}$$

This analysis is more transparent, however, if we use $k_p$ rather than $\omega_p$ as a relevant variable. Then, from (1.1),

$$d\omega_p = \frac{\partial\omega_p}{\partial k_p}\, dk_p + \frac{\partial\omega_p}{\partial D}\, dD. \tag{3.9}$$

From (1.1), the partial derivatives are

$$\frac{\partial\omega_p}{\partial k_p} = \frac{\omega_p}{2}\left[\frac{1}{k_p} + \frac{D\,\mathrm{sech}^2(k_p D)}{\tanh(k_p D)}\right] \quad \text{and} \tag{3.10}$$

$$\frac{\partial\omega_p}{\partial D} = \frac{\omega_p k_p\,\mathrm{sech}^2(k_p D)}{2\tanh(k_p D)}. \tag{3.11}$$

Substituting (3.10) and (3.11) into (3.9) and this result into (3.8) gives

$$\begin{aligned} d(\ln\omega_*) = {} & \frac{1}{2k_p}\left[1 + \frac{k_p D\,\mathrm{sech}^2(k_p D)}{\tanh(k_p D)}\right] dk_p \\ & + \frac{du_*}{u_*} + \frac{k_p\,\mathrm{sech}^2(k_p D)}{2\tanh(k_p D)}\, dD. \end{aligned} \tag{3.12}$$

To simplify the subsequent analysis, I rewrite (3.12) as

$$d(\ln\omega_*) = C_{\omega1}\, dk_p + C_{\omega2}\, du_* + C_{\omega3}\, dD, \tag{3.13}$$

where

$$C_{\omega1} = \frac{1}{2}\left[\frac{1}{k_p} + \frac{D\,\mathrm{sech}^2(k_p D)}{\tanh(k_p D)}\right], \tag{3.14a}$$

$$C_{\omega2} = \frac{1}{u_*}, \quad \text{and} \tag{3.14b}$$

$$C_{\omega3} = \frac{k_p\,\mathrm{sech}^2(k_p D)}{2\tanh(k_p D)}. \tag{3.14c}$$

In (3.13), I interpret the differentials as deviations from their respective means and the $C$ coefficients as averages over the entire DMAJ dataset. Consequently, under the assumption that $k_p$, $u_*$, and $D$ are not correlated with each other, I square (3.13) and average to compute the variance of $\ln\omega_*$:

$$\begin{aligned} \sigma^2_{\ln\omega_*} &= \overline{d(\ln\omega_*)\, d(\ln\omega_*)} \\ &= C^2_{\omega1}\sigma^2_{k_p} + C^2_{\omega2}\sigma^2_{u_*} + C^2_{\omega3}\sigma^2_D. \end{aligned} \tag{3.15}$$

Here, $\sigma^2$ denotes the variance, the subscripts indicate the relevant variables, and the overbar means an average over the DMAJ dataset. The variances of $k_p$, $u_*$, and $D$ are defined as $\sigma^2_{\ln\omega_*}$ is—as the average of the square of the differentials. Notice that (3.15) includes no terms like cov[$k_p$, $u_*$] under the assumption that none of the fundamental variables are correlated.

Next, consider the differential of the logarithm of $C_{\mathrm{DN},\lambda_p/2}$. From (2.6),

$$d(\ln C_{\mathrm{DN},\lambda_p/2}) = \frac{1}{C_{\mathrm{DN},\lambda_p/2}}\left(\frac{\partial C_{\mathrm{DN},\lambda_p/2}}{\partial k_p}\,dk_p + \frac{\partial C_{\mathrm{DN},\lambda_p/2}}{\partial z_0}\,dz_0\right). \tag{3.16}$$

From (2.6), we easily obtain

$$\frac{\partial C_{\mathrm{DN},\lambda_p/2}}{\partial k_p} = \frac{2C_{\mathrm{DN},\lambda_p/2}}{k_p \ln[\pi/(k_p z_0)]} \quad \text{and} \tag{3.17}$$

$$\frac{\partial C_{\mathrm{DN},\lambda_p/2}}{\partial z_0} = \frac{2C_{\mathrm{DN},\lambda_p/2}}{z_0 \ln[\pi/(k_p z_0)]}. \tag{3.18}$$

Therefore, (3.16) becomes

$$d(\ln C_{\mathrm{DN},\lambda_p/2}) = \frac{2}{\ln[\pi/(k_p z_0)]}\left(\frac{dk_p}{k_p} + \frac{dz_0}{z_0}\right). \tag{3.19}$$

But remember, $z_0$ is not a fundamental variable in this analysis; it derives from $u_*$ and $U_{N10}$ through (2.3). This equation gives

$$dz_0 = \frac{\partial z_0}{\partial u_*}\,du_* + \frac{\partial z_0}{\partial U_{N10}}\,dU_{N10}, \tag{3.20}$$

where

$$\frac{\partial z_0}{\partial u_*} = \frac{\kappa z_0 U_{N10}}{u_*^2} \tag{3.21}$$

and

$$\frac{\partial z_0}{\partial U_{N10}} = -\frac{\kappa z_0}{u_*}. \tag{3.22}$$

Substituting (3.21) and (3.22) into (3.20) and this result, in turn, into (3.19) yields

$$d(\ln C_{\mathrm{DN},\lambda_p/2}) = \frac{2}{\ln[\pi/(k_p z_0)]}\left(\frac{dk_p}{k_p} + \frac{\kappa U_{N10}}{u_*^2}\,du_* - \frac{\kappa}{u_*}\,dU_{N10}\right). \tag{3.23}$$

Again, to make subsequent manipulations more obvious and less cumbersome, I rewrite this as

$$d(\ln C_{\mathrm{DN},\lambda_p/2}) = C_{C1}\,dk_p + C_{C2}\,du_* + C_{C3}\,dU_{N10}, \tag{3.24}$$

where

$$C_{C1} = \frac{2}{k_p \ln[\pi/(k_p z_0)]}, \tag{3.25a}$$

$$C_{C2} = \frac{2\kappa U_{N10}}{u_*^2 \ln[\pi/(k_p z_0)]}, \quad \text{and} \tag{3.25b}$$

$$C_{C3} = -\frac{2\kappa}{u_* \ln[\pi/(k_p z_0)]}. \tag{3.25c}$$

As above, I interpret these $C$ coefficients as averages over the DMAJ dataset and, therefore, estimate the variance of $\ln C_{\mathrm{DN},\lambda_p/2}$ as

$$\sigma^2_{\ln C_{\mathrm{DN},\lambda_p/2}} = \overline{d(\ln C_{\mathrm{DN},\lambda_p/2})\,d(\ln C_{\mathrm{DN},\lambda_p/2})} = C_{C1}^2\sigma_{k_p}^2 + C_{C2}^2\sigma_{u_*}^2 + C_{C3}^2\sigma_{U_{N10}}^2, \tag{3.26}$$

which introduces the variance in $U_{N10}$, $\sigma^2_{U_{N10}}$. Again, (3.26) includes no covariance terms because these are all assumed to be zero.

Equations (3.13) and (3.24) provide the covariance between $\ln C_{\mathrm{DN},\lambda_p/2}$ and $\ln\omega_*$, which then yields the slope a from (3.2). This covariance is

$$\mathrm{cov}[\ln C_{\mathrm{DN},\lambda_p/2}, \ln\omega_*] = \overline{d(\ln C_{\mathrm{DN},\lambda_p/2})\,d(\ln\omega_*)} = C_{\omega1}C_{C1}\sigma_{k_p}^2 + C_{\omega2}C_{C2}\sigma_{u_*}^2 \tag{3.27}$$

and is generally nonzero because both $\sigma_{k_p}^2$ and $\sigma_{u_*}^2$ are positive definite and the $C$s are not all near zero. That is, because $C_{\mathrm{DN},\lambda_p/2}$ and $\omega_*$ are formed from some of the same variables, they have built-in correlation despite the assumption that none of the fundamental variables are correlated.

Figure 2 shows the scatterplot of $C_{\mathrm{DN},\lambda_p/2}$ and $\omega_*$ values from the DMAJ dataset. The plot exhibits a remarkably high correlation coefficient for geophysical data, 0.949.

Least squares regression as represented by (3.1)–(3.3) presumes that the $x$ variable is known perfectly and the $y$ variable contains random uncertainty. In most geophysical datasets, including the DMAJ set, both $x$ and $y$ are uncertain. To acknowledge this fact, I usually calculate three fitting lines: one based on the least squares fit of $y$ versus $x$, a second based on $x$ versus $y$, and the

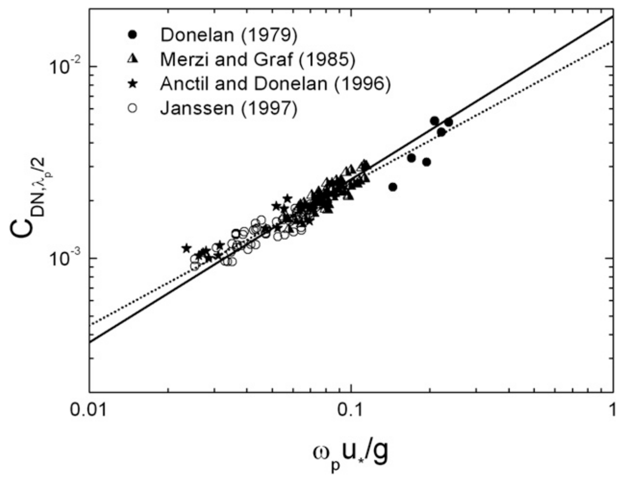


FIG. 2. Scatterplot of the $C_{DN,\lambda_p/2}$ and $\omega_* = \omega_p u_*/g$ values from the DMAJ dataset. The dotted line is the best fit through the data, (3.28), and represents the bisector of $y$ vs $x$ and $x$ vs $y$ least squares fits. The solid line is (3.29) and represents the fictitious correlation, which is based on the assumption that none of the fundamental variables are correlated. The correlation coefficient is 0.949.

bisector of these two lines (e.g., Andreas 2002). That bisector usually represents the linear trend in the data better than either of the former two lines. The dotted line in Fig. 2 is this bisector; its equation is

$$C_{DN,\lambda_p/2} = 0.0136\omega_*^{0.742}. \qquad (3.28)$$

From the equations that I have developed for $\mathrm{cov}[\ln C_{CN,\lambda_p/2}, \ln\omega_*]$, $\sigma^2_{\ln C_{DN,\lambda_p/2}}$, and $\sigma^2_{\ln\omega_*}$ under the assumption that none of the variables in the DMAJ dataset are correlated—namely, (3.27), (3.26), and (3.15), respectively—I can use (3.1)–(3.3) to compute $y$ versus $x$, $x$ versus $y$, and bisector fits that reflect the fictitious correlation. The solid line in Fig. 2 is that bisector; its equation is

$$C_{DN,\lambda_p/2} = 0.0183\omega_*^{0.851}. \qquad (3.29)$$

Figure 2 emphasizes visually what (3.28) and (3.29) tell us: the best fit through the DMAJ data is not very different from a fit that assumes none of the fundamental variables—$k_p$, $u_*$, $U_{N10}$, and $D$—are correlated with each other. The good correlation between $C_{DN,\lambda_p/2}$ and $\omega_*$ evident in Fig. 2 results, largely, from fictitious correlation induced by using the same quantities to create both $x$ and $y$ variables.

Table 1 lists the values that went into my computations of the fictitious correlation. In particular, we see from (3.27) and this table that $\mathrm{cov}[\ln C_{DN,\lambda_p/2}, \ln\omega_*]$ and, thus, the slope must be positive—even with no correlation between independent variables—because $\sigma^2_{k_p}$, $\sigma^2_{u_*}$, $C_{\omega 1}$, $C_{\omega 2}$, $C_{C1}$, and $C_{C2}$ are all positive.

Willmott (1982) used the mean-square error (MSE) to evaluate how well a model represents data. With Fig. 2 as an example, that metric is

$$\mathrm{MSE} = \frac{1}{N}\sum_{i=1}^{N}(y_i - y_{mi})^2, \qquad (3.30)$$

where the $y_i$ are the observations of $\ln C_{DN,\lambda_p/2}$ and the $y_{mi}$ are the model estimates based on

$$\ln C_{DN,\lambda_p/2} = a \ln\omega_* + b. \qquad (3.31)$$

We have two candidates for the model fit, (3.31): one is the log–log version of (3.28), which was obtained by fitting the data (coefficients denoted $a_d$ and $b_d$); the other is the log–log version of (3.29), obtained by evaluating the fictitious correlation (coefficients denoted $a_{fc}$ and $b_{fc}$).

In the appendix, I derive an expression for MSE that works for both of these fits. Table 2 lists the required data.

From Table 2 and (A3), the mean-square error for the data-based fit is $\mathrm{MSE}_d = 0.012\,50$; the mean-square error for the fit based on the fictitious correlation is $\mathrm{MSE}_{fc} = 0.01668$. That is, for this dataset, assuming that $\lambda_p/2$ is a meaningful scaling height for the drag coefficient improves our ability to explain the scatter in the data by only 25% compared to the assumption that none of the variables in $C_{DN,\lambda_p/2}$ and $\omega_*$ are correlated [viz., $(\mathrm{MSE}_d - \mathrm{MSE}_{fc})/\mathrm{MSE}_{fc} = -0.25$].

Another way to evaluate fictitious correlation in a dataset is to randomize the variables (e.g., Hicks 1981; Andreas and Hicks 2002; Klipp and Mahrt 2004; Baas et al. 2006; Mahrt 2008). Because the hypothesis we are discussing is that $\lambda_p$ (or $k_p$) is the relevant length scale for parameterizing air–sea drag, I randomized the $k_p$ values in the DMAJ dataset. In other words, I randomly scrambled all the $k_p$ values in the DMAJ dataset several times while holding $u_*$, $U_{N10}$, and $D$ in position. The $\omega_p$ values in the DMAJ dataset are also now randomized because they are related to $k_p$ through (1.1). In effect, after this scrambling, $k_p$ and $\omega_p$ should be uncorrelated with the other fundamental variables, $u_*$, $U_{N10}$, and $D$, and should have no ability to predict the air–sea drag coefficient.

Figure 3 shows a plot like Fig. 2 but with $C_{DN,\lambda_p/2}$ and $\omega_*$ now calculated from these randomized data. I would expect a fairly scattered plot under normal circumstances; but the plot in Fig. 3 is quite tight, with a correlation coefficient of 0.762. In other words, randomizing $k_p$ has not destroyed the correlation between $C_{DN,\lambda_p/2}$

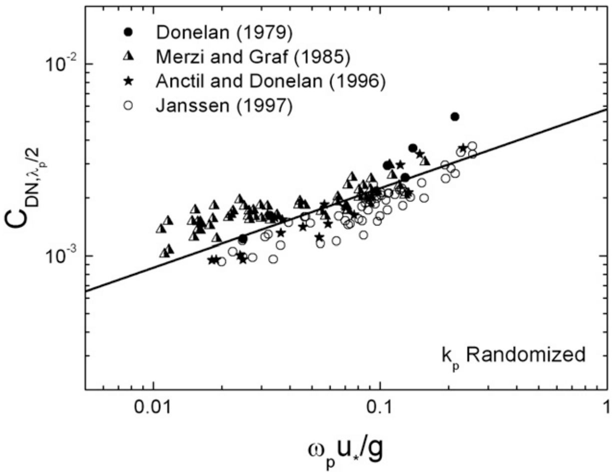


FIG. 3. As in Fig. 2, a scatterplot of $C_{\mathrm{DN},\lambda_p/2}$ vs $\omega_* = \omega_p u_*/g$ from the DMAJ dataset; but, here, the $k_p$ values have been randomized with respect to the other reported variables. Still, the correlation coefficient is 0.762. The line is the best fit to the data, determined as the bisector of $y$ vs $x$ and $x$ vs $y$ fits.

and $\omega_*$, which must be required by the shared variables rather than any underlying physics.

The fitting line in Fig. 3 is immaterial, so I do not give its equation. The standard deviations listed in Table 1 do not change when $k_p$ is randomized; but the coefficients $C_{\omega 1}$, $C_{\omega 3}$, $C_{C1}$, $C_{C2}$, and $C_{C3}$ all do because they include $k_p$ and other independent variables. Consequently, another scrambling of the $k_p$ values in the DMAJ dataset would yield a scatterplot with a different slope than in Fig. 3.

### *b. Plots of $k_p z_0$ versus $\omega_p u_*/g$*

Next, I consider using $k_p$ to nondimensionalize $z_0$: plots of $\ln k_p z_0$ versus $\ln \omega_*$ result. To investigate the fictitious correlation in such plots, I again use differentials. In this case,

$$d(\ln k_p z_0) = \frac{1}{k_p z_0}(z_0\, dk_p + k_p\, dz_0). \tag{3.32}$$

From (3.20)–(3.22), this becomes

$$d(\ln k_p z_0) = \frac{dk_p}{k_p} + \frac{\kappa U_{N10}}{u_*^2}\, du_* - \frac{\kappa}{u_*}\, dU_{N10}. \tag{3.33}$$

To simplify the notation, I rewrite (3.33) as

$$d(\ln k_p z_0) = C_{kz1}\, dk_p + C_{kz2}\, du_* + C_{kz3}\, dU_{N10}, \tag{3.34}$$

where

$$C_{kz1} = \frac{1}{k_p}, \tag{3.35a}$$

TABLE 1. Quantities computed from the DMAJ dataset and used here to assess the fictitious correlation.

| | |
|---|---|
| $\sigma_{k_p}$ | 0.324 m$^{-1}$ |
| $\sigma_{u_*}$ | 0.213 m s$^{-1}$ |
| $\sigma_{U_{N10}}$ | 3.582 m s$^{-1}$ |
| $\sigma_D$ | 7.105 m |
| $C_{\omega 1}$ | 4.433 m |
| $C_{\omega 2}$ | 2.296 s m$^{-1}$ |
| $C_{\omega 3}$ | 0.035 m$^{-1}$ |
| $C_{C1}$ | 1.316 m |
| $C_{C2}$ | 4.527 s m$^{-1}$ |
| $C_{C3}$ | −0.192 s m$^{-1}$ |
| $C_{kz1}$ | 6.588 m |
| $C_{kz2}$ | 22.017 s m$^{-1}$ |
| $C_{kz3}$ | –0.918 s m$^{-1}$ |

$$C_{kz2} = \frac{\kappa U_{N10}}{u_*^2}, \quad \text{and} \tag{3.35b}$$

$$C_{kz3} = -\frac{\kappa}{u_*}. \tag{3.35c}$$

Table 1 also lists these $C_{kz}$ values for the DMAJ dataset.

As before, the variance of $\ln k_p z_0$ is

$$\begin{aligned}\sigma^2_{\ln k_p z_0} &= \overline{d(\ln k_p z_0)\, d(\ln k_p z_0)} \\ &= C^2_{kz1}\sigma^2_{k_p} + C^2_{kz2}\sigma^2_{u_*} + C^2_{kz3}\sigma^2_{U_{N10}},\end{aligned} \tag{3.36}$$

and the covariance between $\ln k_p z_0$ and $\ln \omega_*$ is

$$\begin{aligned}\mathrm{cov}[\ln k_p z_0, \ln \omega_*] &= \overline{d(\ln k_p z_0)\, d(\ln \omega_*)} \\ &= C_{\omega 1} C_{kz1}\sigma^2_{k_p} + C_{\omega 2} C_{kz2}\sigma^2_{u_*}.\end{aligned} \tag{3.37}$$

With these two results and (3.15), I can compute the fictitious correlation in a plot of $\ln k_p z_0$ versus $\ln \omega_*$. Notice, with the values listed in Table 1, (3.37) requires a large, positive value of cov[$\ln k_p z_0$, $\ln \omega_*$] and, thus, a positive slope despite no assumed correlation between any variables.

Figure 4 shows a scatterplot of the $k_p z_0$ and $\omega_*$ values in the DMAJ dataset. Again, the correlation is tight; the correlation coefficient is 0.949. As in Fig. 2, the dotted line in the figure is the bisector of least squares fits of $y$ versus $x$ and $x$ versus $y$. Its equation is

$$k_p z_0 = 3.071\omega_*^{3.503}. \tag{3.38}$$

The solid line in Fig. 4 shows the fictitious correlation in the data according to the equations that I have derived in this and in section 3a. Again, this line is the bisector of the $y$ versus $x$ and $x$ versus $y$ fictitious fits and is

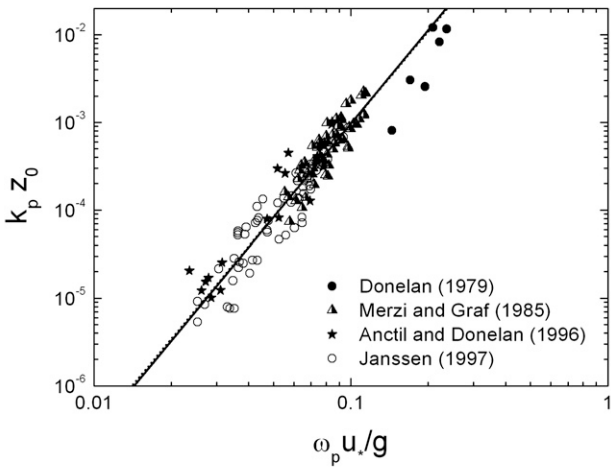


FIG. 4. Scatterplot of the $k_p z_0$ and $\omega_* = \omega_p u_*/g$ values from the DMAJ dataset. The dotted line (almost hidden by the solid line) is the best fit through the data, (3.38). The solid line is (3.39) and represents the fictitious correlation, which is based on the assumption that none of the fundamental variables are correlated. The correlation coefficient is 0.949.

$$k_p z_0 = 3.431\omega_*^{3.544}. \qquad (3.39)$$

In Fig. 4, this result almost hides the dotted line, which is based on regressing the actual data. Again, I conclude that shortcomings in the DMAJ dataset create severe fictitious correlation in plots of nondimensional variables. The dataset is therefore inadequate for studying how air–sea momentum transfer depends on $k_p$.

To emphasize this conclusion, I look at the mean-square errors in predictions of $\ln k_p z_0$ based on the fit to the data, (3.38), and the fit required by the fictitious correlation, (3.39). I again use the MSE as defined by (3.30), a log–log representation that is now

$$y_m = \ln k_p z_0 = a \ln\omega_* + b. \qquad (3.40)$$

I also use the equations derived in the appendix and the values in Table 2.

For the data in Fig. 4, the mean-square error for the data-based fit is $\mathrm{MSE}_d = 0.2809$. For the fit that reflects only fictitious correlation, the mean-square error is $\mathrm{MSE}_{\mathrm{fc}} = 0.2844$. The hypothesis that $k_p$ is a useful scale for nondimensionalizing $z_0$, thus, receives little support from this figure: the $k_p$ scaling explains the scatter in the data only 1.2% better than the fit that assumes none of the variables in $k_p z_0$ and $\omega_*$ are correlated [i.e., $(\mathrm{MSE}_d - \mathrm{MSE}_{\mathrm{fc}})/\mathrm{MSE}_{\mathrm{fc}} = -0.012$].

Finally, I show in Fig. 5 a plot like Fig. 4; but here the $k_p$ values in the DMAJ dataset are randomly scrambled, as before. In typical geophysical datasets, such scrambling would produce a truly scattered scatterplot; but Fig. 5 still shows fairly good correlation between $k_p z_0$ and $\omega_*$. The correlation coefficient is 0.756. The variables that $k_p z_0$ and $\omega_*$ share—namely, $k_p$ and $u_*$—simply require a large, positive covariance between $\ln k_p z_0$ and $\ln\omega_*$ regardless of the presence or absence of underlying physics.

As with Fig. 3, the equation for the fitting line in Fig. 5 is immaterial because some of the coefficients used to determine it—namely, $C_{\omega 1}$ and $C_{\omega 3}$—change each time $k_p$ is scrambled.

TABLE 2. Quantities computed from the DMAJ dataset that are used to evaluate the mean-square error in the log–log fits based on the data and on strictly fictitious correlation.

| | |
|---|---|
| $N$ | 142 |
| $\sigma^2_{\ln\omega_*}$ | 0.1982 |
| $\sigma^2_{\ln C_{\mathrm{DN},\lambda_p/2}}$ | 0.1090 |
| $\sigma^2_{\ln k_p z_0}$ | 2.4383 |
| $\mathrm{cov}[\ln C_{\mathrm{DN},\lambda_p/2}, \ln\omega_*]$ | 0.1385 |
| $\mathrm{cov}\,[\ln k_p z_0, \ln\omega_*]$ | 0.6548 |
| $a_d$ for $\ln C_{\mathrm{DN},\lambda_p/2} - \ln\omega_*$ fit | 0.7419 |
| $a_{\mathrm{fc}}$ for $\ln C_{\mathrm{DN},\lambda_p/2} - \ln\omega_*$ fit | 0.8508 |
| $a_d$ for $\ln k_p z_0 - \ln\omega_*$ fit | 3.5032 |
| $a_{\mathrm{fc}}$ for $\ln k_p z_0 - \ln\omega_*$ fit | 3.5438 |

## 4. Conclusions

Fictitious correlation can be insidious. Here I have used the DMAJ dataset, which includes measurements

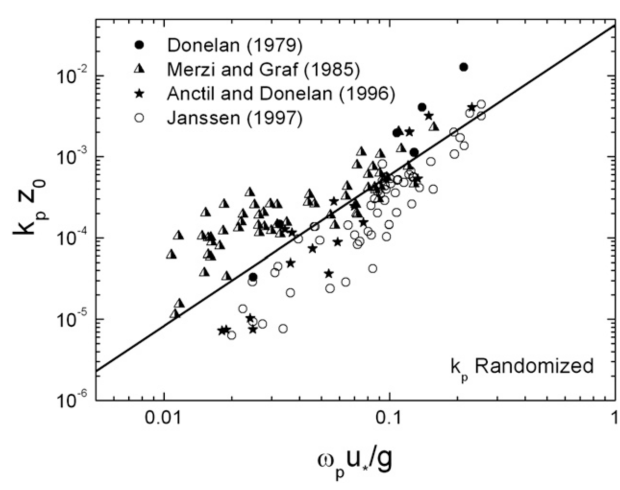


FIG. 5. As in Fig. 4, a scatterplot of $k_p z_0$ vs $\omega_* = \omega_p u_*/g$. But here, the $k_p$ values in the DMAJ dataset have been randomized with respect to the other variables. Nevertheless, the data still have a correlation coefficient of 0.756. The line is the best fit to the data, determined as the bisector of the least squares $y$ vs $x$ and $x$ vs $y$ fits.

of air–sea momentum exchange and wave variables, to demonstrate three distinct points related to fictitious correlation. This dataset has been used in previous studies to investigate the utility of parameterizing air–sea momentum exchange in terms of the peak wavelength of the wind–wave wavenumber spectrum $\lambda_p$. The nondimensional quantities of interest are the neutral-stability drag coefficient evaluated at a height of $\lambda_p/2$, $C_{\mathrm{DN},\lambda_p/2}$, and the roughness length $z_0$ nondimensionalized with $k_p$ ($=2\pi/\lambda_p$), $k_p z_0$. Both $C_{\mathrm{DN},\lambda_p/2}$ and $k_p z_0$ are presumed to be predicted by another nondimensional variable, $\omega_* = \omega_p u_*/g$, where $\omega_p$ is the radian frequency of the peak of the wave frequency spectrum.

My first point has been to suggest warning signs and then to demonstrate techniques for evaluating fictitious correlation, with the DMAJ dataset as an example. First, the dependent variables of interest, $C_{\mathrm{DN},\lambda_p/2}$ and $k_p z_0$, both share $u_*$ with the independent variable $\omega_*$. Moreover, because the DMAJ dataset does not include independent measurements of the required variables $\lambda_p$ and $\omega_p$, $\lambda_p$ (i.e., $k_p$) had to be calculated from the measurements of $\omega_p$ through the wave dispersion relation. As a result, all three nondimensional variables also share $\omega_p$. The potential for fictitious correlation in these analyses is therefore high.

I have derived equations to quantify the effects of the fictitious correlation created by the shared variables. In brief, the equations predict the least squares fits of $\ln C_{\mathrm{DN},\lambda_p/2}$ versus $\ln\omega_*$ and of $\ln k_p z_0$ versus $\ln\omega_*$ under the assumption that none of the fundamental variables—$k_p$, $u_*$, $U_{N10}$, and $D$—are correlated. In contrast, an implicit assumption of wavelength scaling is that $k_p$ must be correlated with some of these other variables.

In log–log plots of both $C_{\mathrm{DN},\lambda_p/2}$ versus $\omega_*$ and $k_p z_0$ versus $\omega_*$, the fitting lines based on my analysis of the fictitious correlation (i.e., assuming uncorrelated variables) are not very different from the best fitting lines through the data. The nondimensional plots are, thus, seriously contaminated by fictitious correlation.

My analysis of the mean-square error in model fits that are based on the data and on the assumption that the only correlation results from the shared variables—the fit based on fictitious correlation—reiterated this conclusion. For the $\ln C_{\mathrm{DN},\lambda_p/2}$ versus $\ln\omega_*$ data, the mean-square error based on $\lambda_p/2$ scaling was only 25% less than the mean-square error based on the assumption of no correlation among variables. For the $\ln k_p z_0$ versus $\ln\omega_*$ data, $k_p$ scaling improved the mean-square error by just 1.2%.

Because the premise in these analyses is that $k_p$ is a fundamental parameter of air–sea momentum exchange, as a third approach to studying the fictitious correlation, I randomized the $k_p$ values in the DMAJ dataset. Because $k_p$ and $\omega_p$ are related in the DMAJ dataset through the dispersion relation, this process also made $\omega_p$ uncorrelated with all the other variables except $k_p$.

Nevertheless, log–log plots of $C_{\mathrm{DN},\lambda_p/2}$ versus $\omega_*$ and $k_p z_0$ versus $\omega_*$ from this randomized set still exhibit good correlation. Correlation coefficients for both plots imply that $\omega_*$ explains at least 50% of the variance of $C_{\mathrm{DN},\lambda_p/2}$ and of $k_p z_0$. Hence, again, the shared variables rather than any underlying physics explain why $C_{\mathrm{DN},\lambda_p/2}$ and $k_p z_0$ are so well correlated with $\omega_p u_*/g$ in the DMAJ dataset.

The second point of my analysis is to establish that another interpretation exists for the results that Hwang (2004, 2005a,b,c) published. He concluded that wavelength scaling is a useful concept by showing that both $C_{\mathrm{DN},\lambda_p/2}$ and $k_p z_0$ are well correlated with $\omega_*$. My reanalysis of the DMAJ dataset suggests, however, that Hwang's finding are dominated by fictitious correlation and, thus, do not establish the validity of wavelength scaling.

The third point of my analysis, therefore, is that future attempts to validate wavelength scaling should include direct measurements of $\lambda_p$. In particular, $C_{\mathrm{DN},\lambda_p/2}$, $k_p z_0$, and $\omega_*$ already share $u_*$. If $\lambda_p$ has not been measured but must be estimated from $\omega_p$ or $c_p$, these three nondimensional variables also share $\omega_p$. Figures 2–5 demonstrate how badly we can be misled by fictitious correlation in such circumstances and, thus, argue for forming nondimensional variables from only independent observations.

*Acknowledgments.* I thank Paul Hwang for providing me a copy of the DMAJ dataset; Fabrice Veron and Michael Banner for helpful discussions about wave mechanics; Bill Plant for sharing the preprint of his proof that $k_p$ and $\omega_p$ are not related by the dispersion relation; Jerry Smith, my *JPO* editor, for offering advice on better focusing the manuscript; and an anonymous reviewer for fair and useful comments. The Office of Naval Research supported this work with Grant N00014-08-1-0411.

## APPENDIX

### Estimates of the Mean-Square Error

A general least squares linear regression model is

$$y_m = ax + b, \tag{A.1}$$

where $x$ is an observation and $y_m$ is the corresponding model prediction. Although for both Figs. 2 and 4 I obtained $a$ as a bisector of $y$ versus $x$ and $x$ versus $y$ fits, $b$ still derives from (3.3). Substituting (A.1) and (3.3) into the definition of the mean-square error (3.30) thus yields

$$\mathrm{MSE} = \frac{1}{N}\sum_{i=1}^{N}[(y_i - \overline{y}) - a(x_i - \overline{x})]^2. \qquad (A.2)$$

Expanding the square in (A.2) finally leads to

$$\mathrm{MSE} = \frac{N-1}{N}(\sigma_y^2 - 2a\,\mathrm{cov}[x, y] + a^2\sigma_x^2). \qquad (A.3)$$

Here, the $N - 1$ occurs because $\sigma_x^2$, $\sigma_y^2$, and $\mathrm{cov}[x, y]$ are unbiased estimators of the $x$ and $y$ variances and the covariance between $x$ and $y$, respectively.

Equation (A.3) is accurate regardless of whether the coefficients $a$ and $b$ in (A.1) derive from fitting the data or from assuming only fictitious correlation. Hence, (A.3) is what I use to evaluate the mean-square error for the various fits discussed in section 3. Table 2 lists the slopes for both the data-based fits ($a_d$) and the fits implied by fictitious correlation ($a_{\mathrm{fc}}$).

## REFERENCES


Al-Zanaidi, M. A., and W. H. Hui, 1984: Turbulent airflow over water waves—A numerical study. *J. Fluid Mech.,* **148,** 225–246.

Anctil, F., and M. A. Donelan, 1996: Air-water momentum flux observations over shoaling waves. *J. Phys. Oceanogr.,* **26,** 1344–1353.

Andreas, E. L, 2002: Parameterizing scalar transfer over snow and ice: A review. *J. Hydrometeor.,* **3,** 417–432.

——, and B. B. Hicks, 2002: Comments on "Critical test of the validity of Monin–Obukhov similarity during convective conditions." *J. Atmos. Sci.,* **59,** 2605–2607.

——, K. J. Claffey, R. E. Jordan, C. W. Fairall, P. S. Guest, P. O. G. Persson, and A. A. Grachev, 2006: Evaluations of the von Kármán constant in the atmospheric surface layer. *J. Fluid Mech.,* **559,** 117–149.

Baas, P., G. J. Steeneveld, B. J. H. van de Wiel, and A. A. M. Holtslag, 2006: Exploring self-correlation in flux-gradient relationships for stably stratified conditions. *J. Atmos. Sci.,* **63,** 3045–3054.

Donelan, M. A., 1979: On the fraction of wind momentum retained by waves. *Marine Forecasting: Predictability and Modelling in Ocean Hydrodynamics,* J. C. J. Nihoul, Ed., Elsevier, 141–159.

——, and W. J. Pierson Jr., 1987: Radar scattering and equilibrium ranges in wind-generated waves with application to scatterometry. *J. Geophys. Res.,* **92,** 4971–5029.

Hicks, B. B., 1978a: Some limitations of dimensional analysis and power laws. *Bound.-Layer Meteor.,* **14,** 567–569.

——, 1978b: Comments on "The characteristics of turbulent velocity components in the surface layer under convective conditions," by H. A. Panofsky, H. Tennekes, D. H. Lenschow, and J. C. Wyngaard. *Bound.-Layer Meteor.,* **15,** 255–258.

——, 1981: An examination of turbulence statistics in the surface boundary layer. *Bound.-Layer Meteor.,* **21,** 389–402.

Hwang, P. A., 2004: Influence of wavelength on the parameterization of drag coefficient and surface roughness. *J. Oceanogr.,* **60,** 835–841.

——, 2005a: Comparison of ocean surface wind stress computed with different parameterization functions of the drag coefficient. *J. Oceanogr.,* **61,** 91–107.

——, 2005b: Drag coefficient, dynamic roughness and reference wind speed. *J. Oceanogr.,* **61,** 399–413.

——, 2005c: Temporal and spatial variation of the drag coefficient of a developing sea under steady wind-forcing. *J. Geophys. Res.,* **110,** C07024, doi:10.1029/2005JC002912.

——, 2006: Duration- and fetch-limited growth functions of wind-generated waves parameterized with three different scaling wind velocities. *J. Geophys. Res.,* **111,** C02005, doi:10.1029/2005JC003180.

Janssen, J. A. M., 1997: Does wind stress depend on sea-state or not? A statistical error analysis of HEXMAX data. *Bound.-Layer Meteor.,* **83,** 479–503.

Kenney, B. C., 1982: Beware of spurious self-correlations! *Water Resour. Res.,* **18,** 1041–1048.

Klipp, C. L., and L. Mahrt, 2004: Flux-gradient relationship, self-correlation and intermittency in the stable boundary layer. *Quart. J. Roy. Meteor. Soc.,* **130,** 2087–2103.

Mahrt, L., 2008: Bulk formulation of surface fluxes extended to weak-wind stable conditions. *Quart. J. Roy. Meteor. Soc.,* **134,** 1–10.

Margenau, H., and G. M. Murphy, 1956: *The Mathematics of Physics and Chemistry*. Van Nostrand, 604 pp.

Massel, S. R., 2007: *Ocean Waves Breaking and Marine Aerosol Fluxes*. Springer, 323 pp.

Merzi, N., and W. H. Graf, 1985: Evaluation of the drag coefficient considering the effects of mobility of the roughness elements. *Ann. Geophys.,* **3,** 473–478.

Oost, W. A., G. J. Komen, C. M. J. Jacobs, and C. van Oort, 2002: New evidence for a relation between wind stress and wave age from measurements during ASGAMAGE. *Bound.-Layer Meteor.,* **103,** 409–438.

Pearson, K., 1897: Mathematical contributions to the theory of evolution—On a form of spurious correlation which may arise when indices are used in the measurement of organs. *Proc. Roy. Soc. London,* **60,** 489–498.

——, A. Lee, and E. M. Elderton, 1910: On the correlation of death-rates. *J. Roy. Stat. Soc.,* **73,** 534–539.

Pierson, W. J., Jr., 1990: Dependence of radar backscatter on environmental parameters. *Surface Waves and Fluxes,* G. L. Geernaert and W. J. Plant, Eds., Vol. II, Kluwer, 173–220.

Plant, W. J., 2009: The ocean wave height variance spectrum: Wavenumber peak versus frequency peak. *J. Phys. Oceanogr.,* **39,** 2382–2383.

——, W. C. Keller, and K. Hayes, 2005: Simultaneous measurement of ocean winds and waves with an airborne coherent real aperture radar. *J. Atmos. Oceanic Technol.,* **22,** 832–846.

Resio, D. T., V. R. Swail, R. E. Jensen, and V. J. Cardone, 1999: Wind speed scaling in fully developed seas. *J. Phys. Oceanogr.,* **29,** 1801–1811.

Tucker, M. J., and E. G. Pitt, 2001: *Waves in Ocean Engineering*. Elsevier, 521 pp.

Willmott, C. J., 1982: Some comments on the evaluation of model performance. *Bull. Amer. Meteor. Soc.,* **63,** 1309–1313.